

NASA Technical Memorandum 104578

A Computer Program for Predicting Oceanic Tidal Currents

D. E. Cartwright and R. D. Ray
Hughes STX Corporation
Lanham, Maryland

B. V. Sanchez
Goddard Space Flight Center
Greenbelt, Maryland



National Aeronautics and
Space Administration

Goddard Space Flight Center
Greenbelt, Maryland 20771



Summary

A computer model is developed for predicting depth-averaged tidal currents from a high-degree spherical harmonic expansion of the elevation field for any diurnal or semidiurnal harmonic constituent. Local friction is ignored, but loading and self-attraction potentials are fully allowed for by use of sequences of Love numbers. Critical latitudes for diurnal tides are covered by direct evaluation of the cyclonic component of current, and linear interpolation of the anti-cyclonic component within $\pm 5^\circ$ of latitude.

Results agree reasonably well with selected measurements of M_2 currents and with M_2 currents computed within Schwiderski's model. However, the Cartwright-Ray model apparently gives noisier results for M_2 and is unacceptably noisy for diurnal constituents. Predictions from either model become unreliable within about 500 km of the coast, but in the open ocean use of our method applied to the Schwiderski maps probably yields a prediction accuracy in the region $5\text{--}10 \text{ mm s}^{-1}$.

PRECEDING PAGE BLANK NOT FILMED

Contents

1	Introduction	1
2	Spherical harmonic formulation	1
3	Rotary components of current and critical latitudes	5
4	Data for verification	7
5	Global M_2 results in the Pacific Ocean	10
6	Detailed comparisons along 140°W	15
7	Description of computer software	17
8	Conclusions	20
	References	21

1 Introduction

Cartwright and Ray (1990, 1991) described how digital arrays of tidal surface elevations of all diurnal and semidiurnal harmonic constituents over most of the world's oceans and seas between $\pm 69^\circ$ latitude were defined by analysis of Geosat altimetry. Many maps of these elevation fields and lists of their spherical harmonic coefficients were presented in Cartwright, Ray, and Sanchez (1991), together with maps of differences between these elevations and the dynamically interpolated elevations of Schwiderski (1983). In this report we describe programs for converting tidal elevation fields to fields of depth-averaged (barotropic) tidal currents, including prediction (or hindcast) currents for arbitrary position and time. The program uses the high-degree spherical harmonic expansions of the elevation field, and may be applied to either the Cartwright-Ray model or the Schwiderski model.

Motivation for developing this program stems from increasing requests for information on tidal currents for various applications. One application is to support estimates of high frequency variability of Earth rotation, whose tidal elements depend on tidal variations in moment of inertia and horizontal momentum (Brosche et al., 1991). Another application is to acoustic thermometry of the ocean (Munk and Forbes, 1989), where the time of travel of acoustic signals over several thousand kilometers is monitored to high precision with a view to detecting climatic changes in mean ocean temperature. Variations in travel time due to tidal currents at all parts of the transmission path are appreciable, and require correction. The required information is at present inadequate or totally lacking.

2 Spherical harmonic formulation

Let (θ, ϕ, t) denote colatitude, east longitude, and time, and $u(\theta, \phi, t)$, $v(\theta, \phi, t)$ the components of horizontal velocity in the directions of increasing θ and ϕ , that is towards south and east, respectively. u and v are related to the

gradients of elevation of the free surface ζ relative to the earth tide by the equations:

$$u_t - 2v\Omega \cos \theta = -(g/a) \left[\zeta - \tilde{\zeta} - \sum_n \gamma'_n \alpha_n \zeta_n \right]_{\theta} \quad (1)$$

$$v_t + 2u\Omega \cos \theta = -(g/a \sin \theta) \left[\zeta - \tilde{\zeta} - \sum_n \gamma'_n \alpha_n \zeta_n \right]_{\phi} \quad (2)$$

where Ω , g , a are the Earth's sidereal rotation frequency, mean surface gravity, and mean radius, respectively, $\tilde{\zeta}$ is the 'equilibrium tide,' and suffices θ , ϕ , t denote differentials. $\tilde{\zeta}$ is also written $\gamma_2 U/g$, where $U(\theta, \phi, t)$ is the known primary tide-generating potential of degree 2 and $\gamma_2 = 1 + k_2 - h_2 = 0.692$ is the reduction factor due to the elastic distortion of the solid Earth. Finally, the summed terms in square brackets are with respect to the degree n of the spherical harmonic expansion ζ_n of the ocean tide ζ , and represents the combined effect of loading and self-attraction. Here, $\gamma'_n = 1 + k'_n - h'_n$ are the loading Love numbers for a spherical shell (Farrell, 1972) and

$$\alpha_n = 0.5629/(2n + 1)$$

includes the ocean: Earth mean density ratio.

Since $\zeta = \sum_n \zeta_n$, the square brackets in (1,2) can also be written

$$\left[\sum_n (1 - \gamma'_n \alpha_n) \zeta_n - \tilde{\zeta} \right]. \quad (3)$$

Many authors of dynamical tide models ignore the loading factors $\gamma'_n \alpha_n$, or effectively set a constant value independent of n (e.g., Schwiderski, 1980). However, loading does supply a significant correction to the gradients of (3), and one advantage of a spherical harmonic expansion of ζ is that it enables us to apply this correction properly. Another advantage is that it simplifies differentiation and interpolation by the use of analytic functions.

Equations (1,2) neglect friction. Friction is of course an important factor in global tidal energetics, but it is well-known to be concentrated in shallow seas. In the deep ocean, any physically plausible representation of bottom friction is easily shown to be two or three orders of magnitude less than other uncertainties in Laplace's equations, and we have therefore neglected it altogether in this application to local currents. The net global effect of friction

is implicit in the known field of $\zeta(\theta, \phi, t)$ and its phases. The physical reality of a dissipative term due to horizontal eddy viscosity, used by Schwiderski (1980) and some other modellers, is dubious and unproven in any practical application.

Following Cartwright, Ray, and Sanchez (1991), our formulation for $\zeta(\theta, \phi, t)$ at major harmonic constituents of frequency ω is

$$\zeta(\theta, \phi, t) = H_1(\theta, \phi) \cos[\omega(t - t_0)] + H_2(\theta, \phi) \sin[\omega(t - t_0)] \quad (4)$$

where

$$H_1(\theta, \phi) = \sum_{n=0}^N \sum_{m=0}^n {}' (a_{nm} \cos m\phi - b_{nm} \sin m\phi) \bar{P}_n^m(\cos \theta) \quad (5)$$

$$H_2(\theta, \phi) = \sum_{n=0}^N \sum_{m=0}^n {}' (c_{nm} \cos m\phi - d_{nm} \sin m\phi) \bar{P}_n^m(\cos \theta) \quad (6)$$

In (4), H_1, H_2 are equivalent to $H(\cos, \sin)G$, where H and G are the conventional constituent amplitude and Greenwich phase lag respectively, and t_0 is an arbitrary time origin at a maximum of the tide potential constituent at the Greenwich meridian—usually near a time of lunar or solar transit. (When applied to real predictions, (4) is modulated by the classical “nodal factors” to account for the position of the Moon’s node in its 18.6-year cycle, excepting purely solar constituents such as P_1 or S_2 .)

In (5,6), $\bar{P}_n^m(\cos \theta)$ is the normalized associated Legendre function (e.g., $\bar{P}_2^2(\cos \theta) = \sqrt{(5/48)} 3 \sin^2 \theta$), and a, b, c, d are arrays of numerical coefficients in millimeters. The prime on the inner summation denotes that the terms for $m = 0$ are halved. N is a large integer appropriate to the spatial resolution of the original data from which the spherical harmonic expansion was evaluated. In the case of the Cartwright-Ray models, $N = 122$.

The Legendre functions are computed from the following recurrence relation:

$$\begin{aligned} \bar{P}_n^m(x) = & \left[\frac{(2n+1)(2n-1)}{(n-m)(n+m)} \right]^{1/2} x \bar{P}_{n-1}^m(x) \\ & - \left[\frac{(2n+1)(n+m-1)(n-m-1)}{(2n-3)(n+m)(n-m)} \right]^{1/2} \bar{P}_{n-2}^m(x). \end{aligned}$$

Unlike some other recurrence relations, this one (recurring upwards on n) is known to be stable (Olver et al., 1983). For computing the derivatives with respect to θ on the right hand side of (1), we used the formula

$$\begin{aligned} \left[\bar{P}_n^m(x) \right]_x (1-x^2) &= -mx \bar{P}_n^m(x) \\ &+ (1-x^2)^{1/2} [(n-m)(n+m+1)]^{1/2} \bar{P}_n^{m+1}(x). \end{aligned}$$

(For $m = n$, the last term is zero.) The ϕ -derivatives in (2) simply involve a slight modification of (5, 6), multiplied by a factor m .

Typical values of the coefficients $(a, b, c, d)_{n,m}$ in the region $n = 120$ are of order 0.01 times typical values in the region $n = 1-10$, so the series for $H_{1,2}$ are reasonably close to convergence above $n = 100$. However, the corresponding series of derivatives H_θ, H_ϕ , being of order $n(a, b, c, d)_{n,m}$ do not converge but remain at about the same order of magnitude up to $n = N$. Accordingly, partial sums of the derivatives up to $N' \leq N$ fluctuate rather widely with choice of N' . We experimented with spatial mean derivatives over an area $(\theta \pm \delta, \phi \pm \delta)$ with $\delta = 2\pi/N'$. This converged better than the series of raw derivatives but still showed unacceptably large variations with N' . Finally, we obtained satisfactory convergence by applying a taper function

$$F_{N'}(n) = \frac{1}{2}(1 + \cos \pi n / (N' + 1)) \quad (7)$$

in the manner of

$$[H_1]_{\theta,\phi} \sim \sum_{n=0}^{N'} \left[F_{N'}(n) \sum_{m=0}^n (a_{nm} \cos m\phi - b_{nm} \sin m\phi) \bar{P}_n^m(\cos \theta) \right]_{\theta,\phi} \quad (8)$$

and $[H_2]_{\theta,\phi}$ similarly. Equation (8) was found to give stable results for derivatives and currents at most ocean locations, except within a few degrees of land, where a sort of Gibbs oscillation induced by the discontinuity to $H = 0$ was still evident.

3 Rotary components of current and critical latitudes

In the detailed solution of (1, 2) we require to express u and v in the same form as (4) with in-phase components u_1, v_1 and quadrature components u_2, v_2 . Pairs (u_1, u_2) and (v_1, v_2) may be converted to amplitudes and phase lags of the south and east components of current in an obvious way. For a constituent of frequency ω , the four components have to satisfy the following equations, derived from (1, 2):

$$\omega u_1 + f v_2 = (g/a)(\xi_2)_\theta = A \quad (9)$$

$$f u_1 + \omega v_2 = -(g/a \sin \theta)(\xi_1)_\phi = B \quad (10)$$

$$\omega u_2 - f v_1 = -(g/a)(\xi_1)_\theta = C \quad (11)$$

$$f u_2 - \omega v_1 = -(g/a \sin \theta)(\xi_2)_\phi = D \quad (12)$$

where f is the coriolis frequency $2\Omega \cos \theta$ and ξ_1, ξ_2 are the in-phase and quadrature components of (3), which on account of (7, 8) is in practice replaced by

$$\xi_1, \xi_2 = \sum_n F_N(n)(1 - \gamma'_n \alpha_n) \zeta_n - \tilde{\zeta}_{1,2}, \quad (13)$$

with $(\zeta_n)_1, (\zeta_n)_2$ defined by the inner terms of (5, 6).

Equations (9-13) also require the derivatives of the equilibrium tide $\tilde{\zeta}$, which are simply given by

$$(\tilde{\zeta}_{1,2})_\theta = 2\gamma_2 H \cos 2\theta (\cos \phi, -\sin \phi) \quad (14)$$

$$(\tilde{\zeta}_{1,2})_\phi = -\gamma_2 H \sin 2\theta (\sin \phi, \cos \phi) \quad (15)$$

for diurnal tides, or by

$$(\hat{\zeta}_{1,2})_\theta = \gamma_2 H \sin 2\theta (\cos 2\phi, -\sin 2\phi) \quad (16)$$

$$(\hat{\zeta}_{1,2})_\phi = \gamma_2 H (\cos 2\theta - 1) (\sin 2\phi, \cos 2\phi) \quad (17)$$

for semidiurnal tides. Here, H is $\sqrt{(15/32\pi)}$ times the amplitude of the chosen harmonic constituent of U/g in the normalization of Cartwright and

Taylor (1971). (Examples of H for epochs around 2000 A.D. are 101.3 (O_1), 142.4 (K_1), 244.1 (M_2), 113.6 (S_2) millimeters.)

Having computed the four quantities A, B, C, D numerically by means of (7, 8, 14, 15) or (7, 8, 16, 17), formal expressions for the velocity components such as

$$u_1 = \frac{\omega A - fB}{\omega^2 - f^2}, \quad u_2 = \frac{\omega C - fD}{\omega^2 - f^2} \quad (18)$$

follow, provided $f \neq \pm\omega$. However, the relations for the *rotary components* of the current are even simpler, and quite useful in other ways. Here we represent the tidal current of frequency ω as the sum of two contrary rotating vectors of amplitude r^+ (positive or anticlockwise rotation) and r^- (clockwise rotation), respectively. In the northern hemisphere, r^+ is also termed a ‘cyclonic’ and r^- an ‘anticyclonic’ rotation, with opposite terminology in the southern hemisphere. Using suffices 1, 2 for the in-phase and quadrature parts as before, one may easily show that

$$2r_1^+ = u_1 + v_2 = \frac{A + B}{\omega + f} \quad (19)$$

$$2r_2^+ = u_2 - v_1 = \frac{C + D}{\omega + f} \quad (20)$$

$$2r_1^- = u_1 - v_2 = \frac{A - B}{\omega - f} \quad (21)$$

$$2r_2^- = -u_2 - v_1 = \frac{D - C}{\omega - f}. \quad (22)$$

The singularities of these equations lie at the “critical latitudes”

$$\theta'_c = 90^\circ - \theta_c = \pm \sin^{-1}(\omega/2\Omega). \quad (23)$$

At the northern (positive) θ'_c , $f = \omega$, so both components of r^- are indeterminate, whereas at the southern (negative) θ'_c , $f = -\omega$ and r^+ is indeterminate. However, the cyclonic rotations are well determined at both critical latitudes. The indeterminacy of the anticyclonic components at $\pm\theta'_c$ stems from the fact that inertial currents have no associated pressure gradient.

For semidiurnal tides, all critical latitudes are poleward of $\theta'_c = 70^\circ$ (74.5° for M_2), outside our present geographical area of interest, but the diurnal θ'_c in the region 26°–30° may not be ignored. Our procedure within ($\theta'_c \pm 5^\circ$) is

to interpolate the anticyclonic rotary component linearly between its values at $\theta'_c + 5^\circ$ and $\theta'_c - 5^\circ$ where computation at typical ocean positions showed its values to be adequately precise. The cyclonic component is computed normally at the correct position. Cartesian current components (u, v) then follow easily from the first equalities of (19–22).

4 Data for verification

The depth-averaged or “barotropic” current is difficult to measure *in situ* on account of variations in the vertical due to internal waves. Current meters record only the current at one or a small number of arbitrary positions in the vertical. Nevertheless, Luyten and Stommel (1991) have recently shown that the mean spectral components at the M_2 frequency over year-long records in ocean depths greater than a kilometer show some consistency from one vertical position to another and partial agreement with barotropic currents extracted by E. W. Schwiderski from his dynamic model. The data presented in Table 1 of Luyten & Stommel (1991) are therefore almost the only source available for verification of our procedure, albeit for the M_2 constituent only.

A rough approximation for other major constituents may be obtained by estimating elevation gradients directly from the published tidal elevation maps of Schwiderski (1983), but accuracy is severely limited by the rounding precision of 1° in phase and 1 cm in amplitude. Besides, such maps are in no way governed by direct measurements of current.

Table 1 shows some comparisons between:

- a. directly recorded M_2 currents selected by Luyten & Stommel (1991) as detailed in their Table 1,
- b. Schwiderski’s M_2 barotropic current at the same site,
- c. current computed by applying our method to a spherical harmonic expansion of Schwiderski’s elevation field, and
- d. current computed by applying our method to the M_2 ocean tide map of Cartwright & Ray (1991), with spherical harmonics as described in Cartwright, Ray, and Sanchez (1991).

Table 1: M_2 current comparisons

		u_o	g_u	v_o	g_v	
1.	Position 31°N, 185°E					
	Observations	(a)	12	39	18	265
	Schwiderski	(b)	13	20	11	265
	This paper	(c)	15	15	13	262
		(d)	18	16	16	266
2.	Position 32°N, 336°E					
	Observations	(a ₁)	24	211	12	27
		(a ₂)	27	168	28	34
	Schwiderski	(b)	24	168	19	18
	This paper	(c)	23	169	22	10
		(d)	26	158	24	8
3.	Position 31°S, 320°E					
	Observations	(a ₁)	24	269	12	34
		(a ₂)	25	268	16	43
		(a ₃)	22	273	18	66
	Schwiderski	(b)	20	263	7	36
	This paper	(c)	22	262	9	20
		(d)	14	258	7	62
4.	Position 0°, 57°E					
	Observations	(a ₁)	4	245	3	300
		(a ₂)	13	268	24	164
	Schwiderski	(b)	11	249	22	128
	This paper	(c)	13	241	23	132
		(d)	13	237	23	128
5.	Position 0°, 212°E					
	Observations	(a ₁)	5	195	11	315
		(a ₂)	4	167	12	308
		(a ₃)	6	200	15	321
		(a ₄)	3	164	11	313
	Schwiderski	(b)	4	153	15	289
	This paper	(c)	4	169	15	290
		(d)	4	157	16	287

Table 2: M₂ current comparisons at 0°, 110°W

		u_o	g_u	v_o	g_v
Observations	(a)	6	266	18	191
Schwiderski	(b)	10	267	22	155
This paper	(c)	10	264	22	154
	(d)	7	248	25	148

The four sites were chosen for the relative agreement between (a) and (b), which is better than average. Where available, observations from other depths at the same site are shown as (a₁), (a₂), etc. The parameters shown are $u_o = \sqrt{u_1^2 + u_2^2}$, $g_u = \arctan(u_2/u_1)$, v_o, g_v similar, in our convention (u south, v east), which differs from the convention used by Luyten and Stommel (1991). Units are mms^{-1} and degrees.

Basically, the variability in the mean M₂ current at different depths at positions 2–5 limits the value of the comparison, but they are probably the best data available. The very low recorded amplitudes at the shallower depth (a₁) at position 4 suggest an instrumental defect; in any case, all computed currents are in fair agreement with the deeper observations (a₂). Elsewhere, all computations are within about 5 mms^{-1} in amplitude and 10° in phase, except for position 3, where our computations with the Cartwright-Ray tidal model (d) are about 10 mms^{-1} lower than the direct observations, though not so different from the Schwiderski data (b). Our computed phase lags (c,d) tend to be slightly less than the observed g_u, g_v , possibly because of our total neglect of local friction.

In Table 2 we make similar comparisons with some current measurements by Weisberg, Halpern, Tang, and Hwang (1987). Their results have special importance because they recorded for 10 months with a heavily instrumented string of ten current meters in a depth of more than 3 km at 0°, 110°W. From the ten simultaneous series the authors were able to separate the barotropic tide from the first three baroclinic modes by dynamic formulae. Monthly estimates of the M₂ barotropic tide show a fair degree of constancy, and their mean values should be more reliable than the single-meter spectral analyses of Luyten and Stommel.

Weisberg *et al.* do not quote values for the Cartesian components u, v , but

specify their mean ellipse in terms of maximum (18.1 mms^{-1}) and minimum (5.9 mms^{-1}) currents and the orientation (91.7°) and phase (6.56 ‘hours’) of one maximum. These figures, together with the information that the current rotates clockwise, may be converted by simple arithmetic to the amplitudes and phases of the rotational components r^+ and r^- , and hence through equations 19–22 to the components u, v listed in row (a) of Table 2. (We have interpreted the given phase as 6.56 *solar* hours; in some contexts lunar hours are used.)

Our three models (b, c, d) agree with each other remarkably well, but comparison with (a) should be judged with less flexibility than in Table 1 on account of the more sophisticated data analysis. In their Figure 7, Weisberg *et al.* compared their mean ellipse with Schwiderski’s computation (equivalent to our ‘b’) and considered that “model and data compare well.” However, one must admit that both data amplitudes are about 20 percent lower than all three models, and, while the u -phases agree well, the data phase lag in v , which is roughly that of the semimajor axis, is some 40° greater than the model results, as is apparent in their Figure 7. It seems possible that the measurements may have been affected by swaying of the mooring line, which would indeed reduce the amplitude, but the discrepancy in g_v should be taken seriously as a suggestion that all three models are insufficiently lagged, at least at this site. Other similar comparisons would, however, be needed to establish this as a fact.

5 Global M_2 results in the Pacific Ocean

Figures 1a and 1b depict the pattern of M_2 tidal currents at 10° intervals of latitude and longitude in the Pacific Ocean, computed with our program from a spherical harmonic expansion of Schwiderski’s map. The expansion is complete to degree 180, but was limited to $N = 120$ in this particular application. The representation used in Figure 1 is novel but complete, and it deserves some preliminary description. At each point, vectors are drawn to represent the rotary components r^+ (bold arrowhead) and r^- (barbed arrowhead) at the time of Greenwich transit t_0 (Equation 4). The direction of r^+ is therefore $\arctan(r_2^+, r_1^+)$ clockwise (negatively) from south, and the direction of r^- is similarly $\arctan(r_2^-, r_1^-)$ in the same sense. The Mercator map projection ensures true directions. The total current vector at t_0 is the

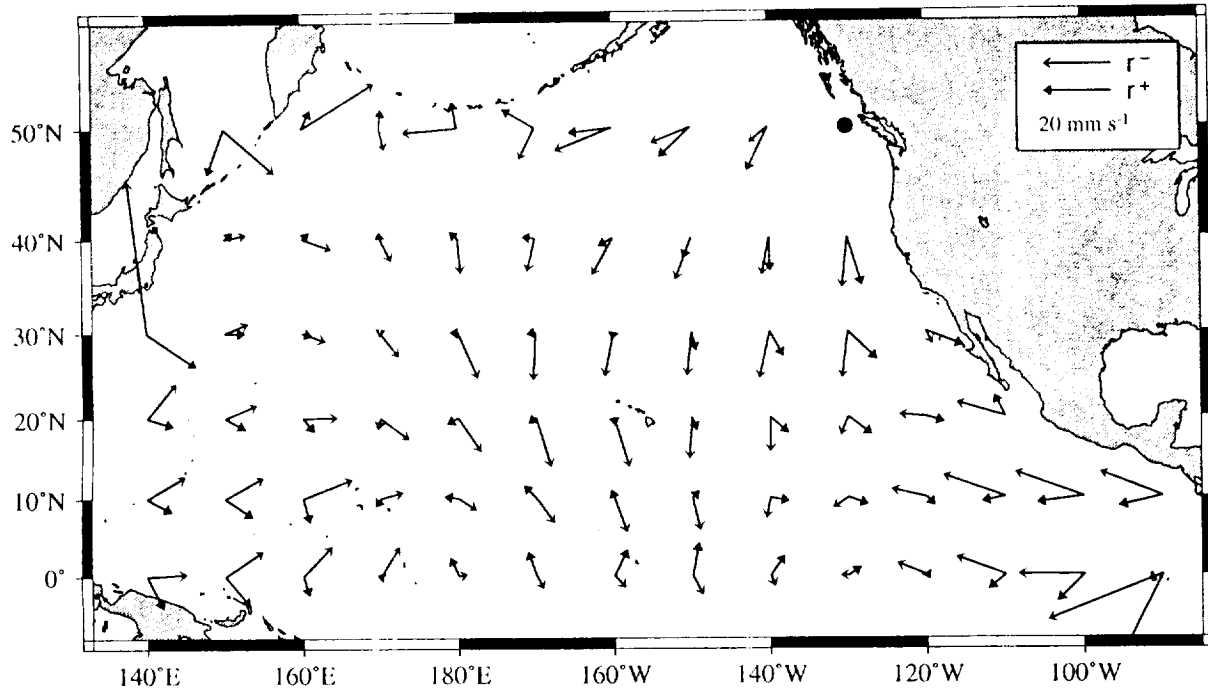


Figure 1a: M_2 rotary current vectors for the North Pacific, computed from tidal elevations of the Schwiderski (1983) model. For interpretation, see text.

vector sum of r^+ and r^- , which may be judged by the parallelogram rule. Black circles are used where one component exceeds 50 mm s^{-1} .

The semimajor axis of each current is the sum of the two amplitudes, along the direction of the bisector of the angle between them. The semiminor axis is the difference, in the direction normal to the bisector. If r^+ and r^- are nearly equal in amplitude, the motion is nearly linear (very thin ellipse). If one has much smaller amplitude than the other, the motion is nearly circular. The sense of rotation is that of the greater amplitude (r^+ anticlockwise, r^- clockwise). All these properties can be assessed by eye.

One readily sees that the sense of rotation is mostly clockwise in the north Pacific and anticlockwise in the south Pacific, as noted globally by Luyten and Stommel (1991–Figure 8). Other features, such as orientation and eccentricity of the ellipses also conform closely with their Figure 8. These characteristics, together with comparisons (b–c) in our Table 1 confirm that our reconstruction of the currents from Schwiderski’s (1983) elevation maps for M_2 is close to his own, although his dynamic formulae differ from our Equations (1–3). It is also interesting to note that our formulation makes no use of ocean depth, which enters only the equation of mass conservation.

Figures 2a and 2b show similar current parameters in the Pacific Ocean,

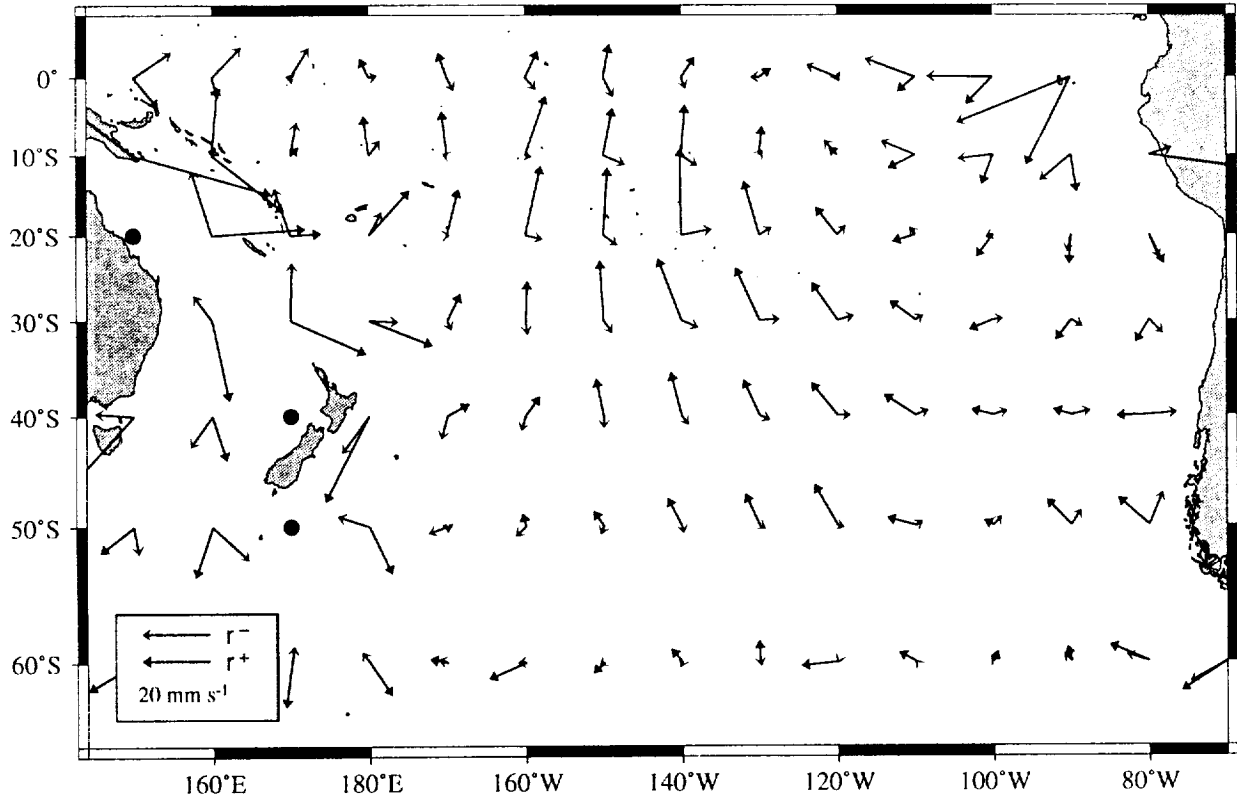


Figure 1b: M_2 rotary current vectors for the South Pacific, computed from tidal elevations of the Schwiderski (1983) model.

from our own model of the M_2 ocean tide, derived from Geosat altimetry with corrections for loading (Cartwright and Ray, 1991; Cartwright, Ray, and Sanchez, 1991). The spherical harmonic analysis is limited by the original data grid to $N = 122$, but we used $N' = 120$ in the computation of currents, for uniformity with Figures 1a, b.

The two pairs of Figures compare very well in most areas, with the notable exception of the most southerly latitude (60°S) where the two elevation maps seem to give quite different results. There are also differences in magnitude in the vicinity of Japan and the Aleutian Islands. The differences in the two maps of M_2 surface elevation are fully discussed in Cartwright and Ray (1991); they are also depicted here as Figure 3. The wide areas of large discrepancy south of New Zealand and west of South America appear not to affect the corresponding currents too strongly, perhaps because the spatial gradients are not greatly affected. The larger differences noted in certain areas of Figures 1 and 2 must be due to differences in short scale structure not easily seen in Figure 3. These will certainly be exaggerated in continental shelf areas of all seas, where both models are too coarse to represent the fine dynamic structure.

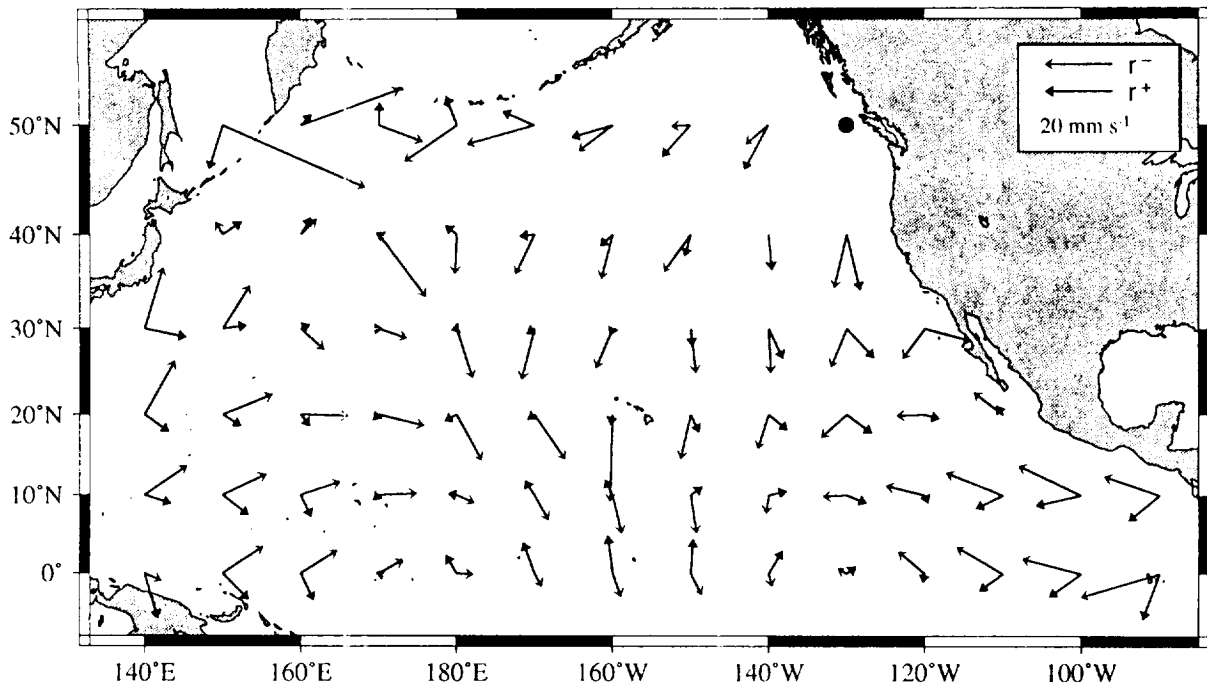


Figure 2a: M_2 rotary current vectors for the North Pacific, computed from tidal elevations of the Cartwright-Ray (1991) model.

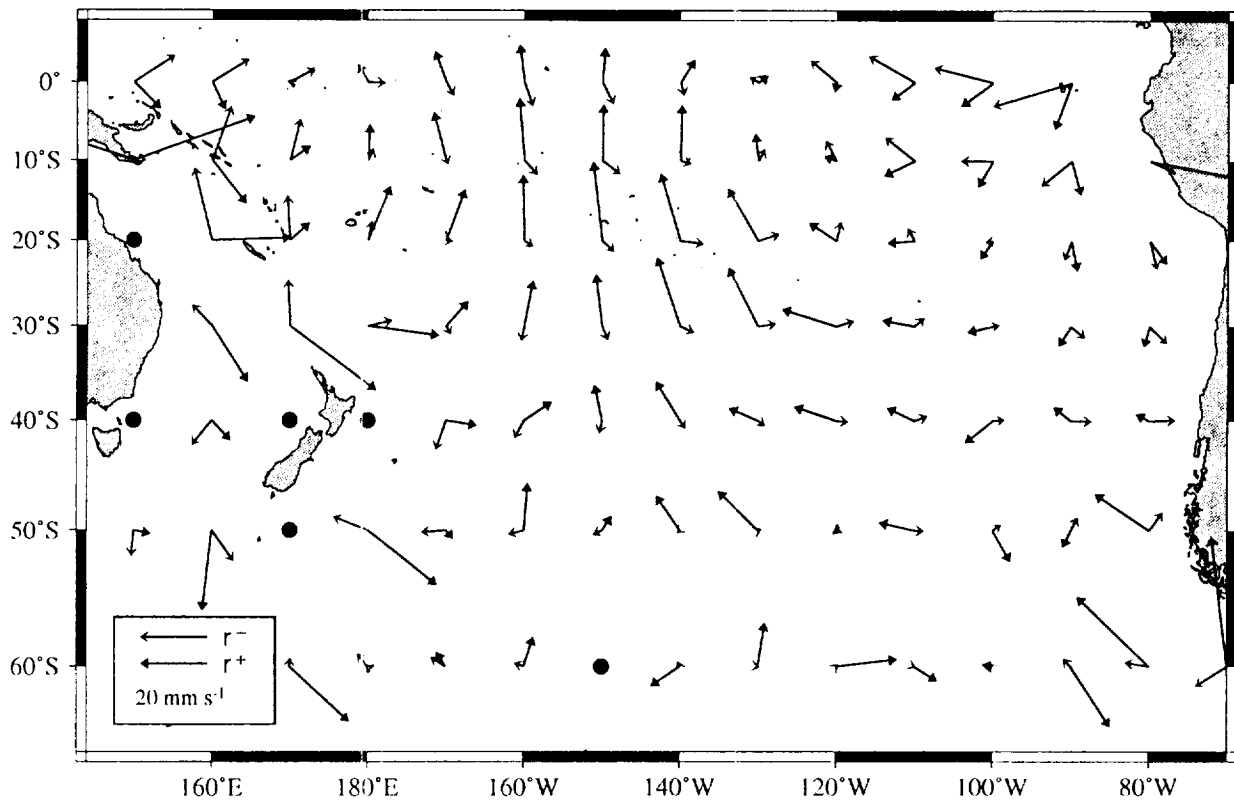
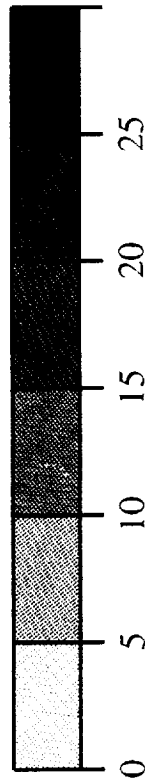
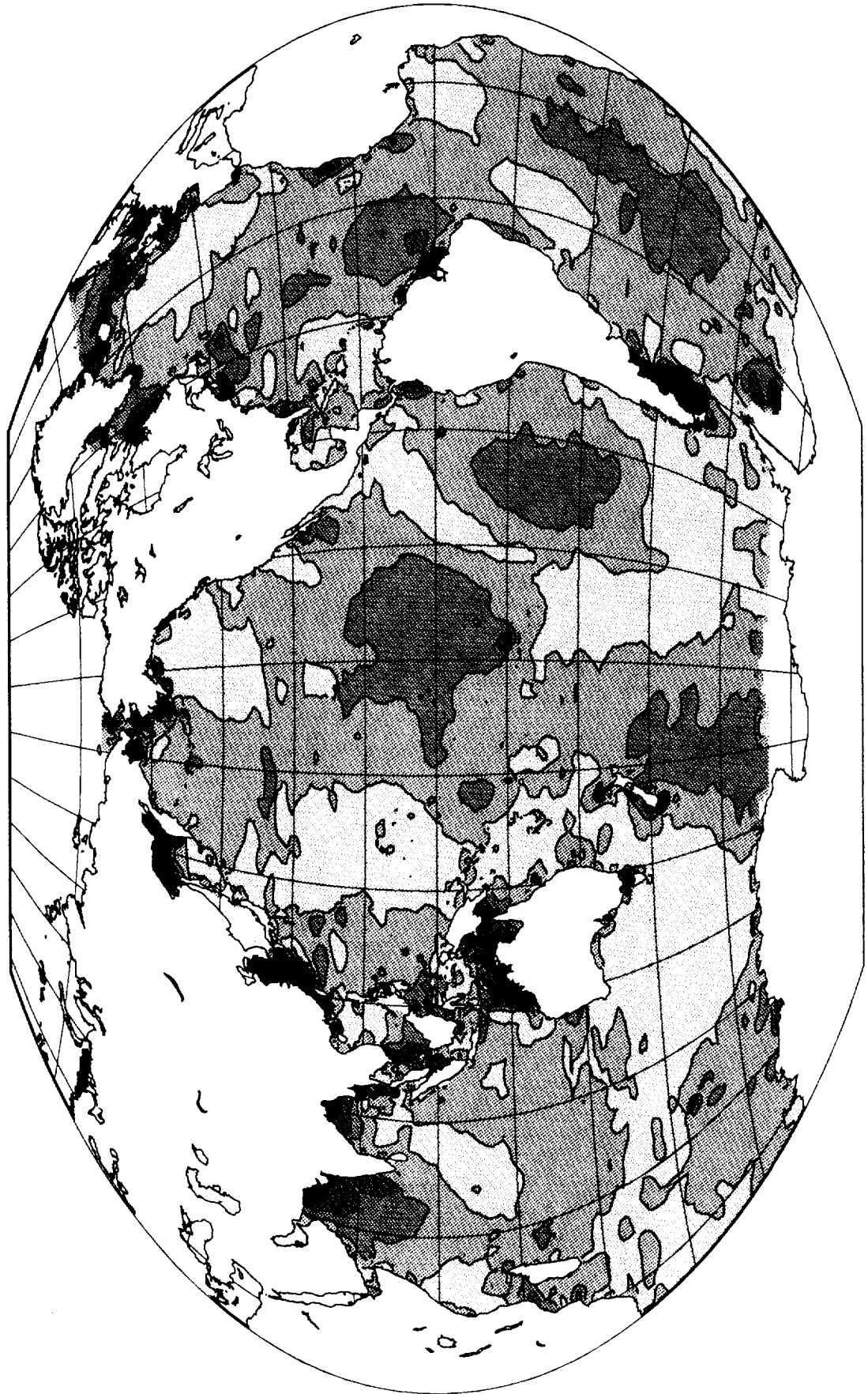


Figure 2b: M_2 rotary current vectors for the South Pacific, computed from tidal elevations of the Cartwright-Ray (1991) model.



6 Detailed comparisons along 140°W

Finally, we compare the results of various computations for the cartesian current components u_1, u_2, v_1, v_2 along the meridian 140°W between the equator and Alaska, at 1° intervals of latitude.

Figure 4a shows the four components plotted from Schwiderski's dynamic model, after correcting a 90° error in the phase lags of the east component. The discontinuities north of 58°N are presumably due to the proximity of shallow shelf seas. The corresponding result of applying our computations to the spherical harmonic expansion of Schwiderski's M_2 elevations is shown in Figure 4b. Only results up to 55°N, with $N' = 120$ are shown. Above 55°N the curves diverge, probably owing to the behaviour of spherical harmonics near the coastal discontinuity. This points to a limitation in the precision of our procedure less than about 500 km from land. In the open ocean, south of latitude 50°, the computation gives a fair representation of the dynamic currents.

Figure 4c shows the results of applying our computation to the Cartwright-Ray M_2 map, also with $N' = 120$. The large wavelength features of all four components are similar to those of Figures 4a and 4b, but there is obviously much short wavelength variation not present in the Schwiderski data. These variations may be real, or they may be merely a reflection of noise in the Cartwright-Ray model. Reducing N' to 60 smoothed out the mid-latitude variations but enhanced the tendency to erratic behaviour at latitude 55°.

Finally, Figures 5, 6, and 7 show the current components for the S_2 constituent and for the diurnal constituents O_1 and K_1 , respectively, obtained by applying our procedures to Schwiderski's (1983) elevation maps. The curves are satisfactorily smooth, with similar dubious behaviour near the coast as observed in M_2 . The diurnal critical latitudes θ'_c are 27.6° (O_1) and 30.0° (K_1), and the effect of the necessary interpolation between $\theta'_c \pm 5^\circ$ discussed

Facing page:

Figure 3: Magnitude of the vector differences between the M_2 vertical elevation models of Schwiderski (1983) and Cartwright and Ray (1991), in cm. The scalar components of these differences can be found in color plates in Cartwright *et al.* (1991). Differences on the Patagonian Shelf exceed 50 cm. Winkel Tripel projection.

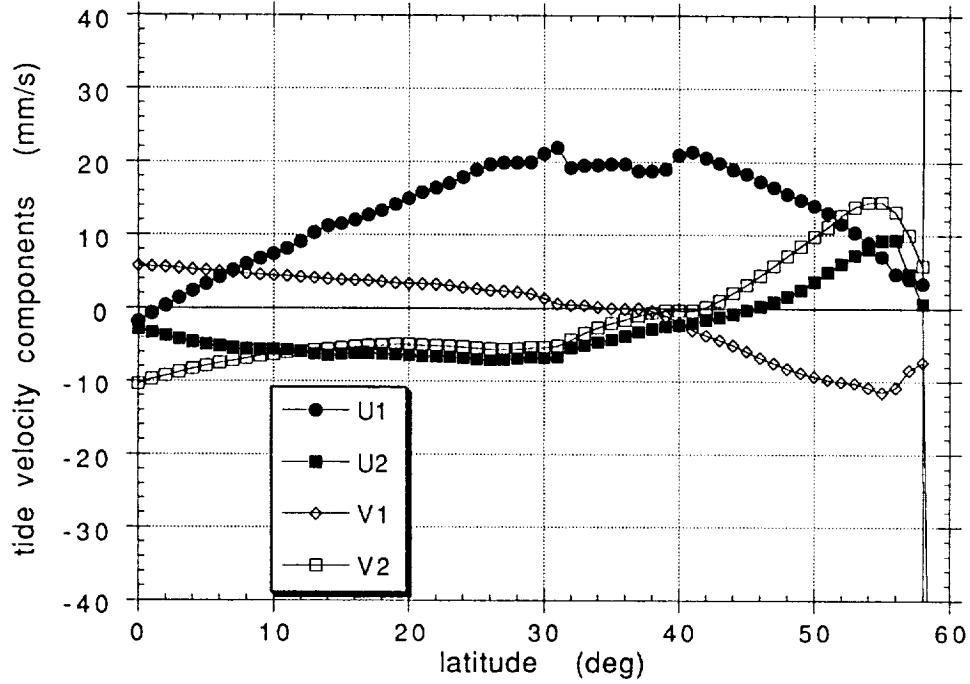


Figure 4a: Cartesian components of the M_2 tidal currents along 140°W , computed by Schwiderski for his global dynamic model.

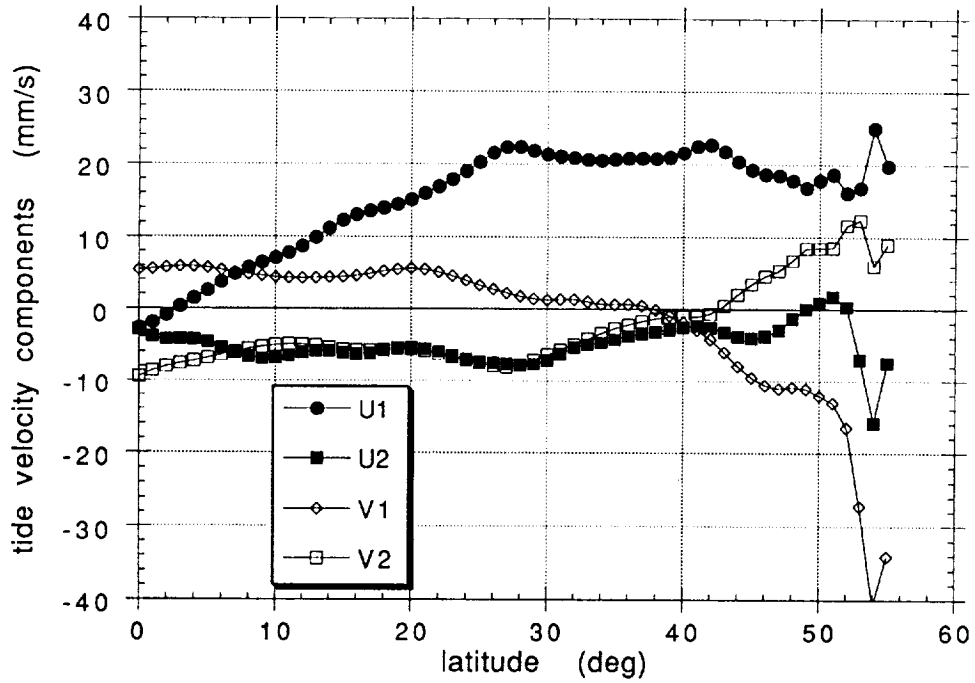


Figure 4b: Cartesian components of the M_2 tidal currents along 140°W , computed here from the tidal elevations of the Schwiderski numerical model.

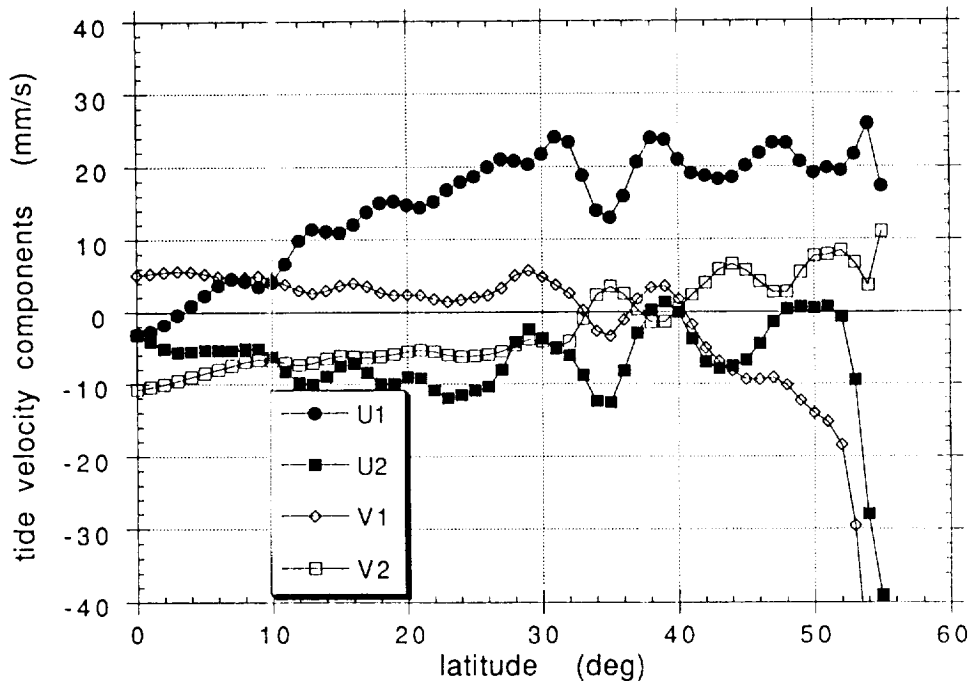


Figure 4c: Cartesian components of the M_2 tidal currents along 140°W , computed here from the tidal elevations of the Cartwright-Ray altimetric model.

in §3 is evident as nearly linear segments of all four curves in these intervals, only the cyclonic rotary components being directly evaluated at every point.

The same procedure was applied to the Cartwright-Ray maps for O_1 and K_1 , but the results contain irregular variations too large for credibility. We conclude that the noise level of our diurnal maps is at present too great to stand the process of differentiation. Until the noise level has been reduced by use of additional altimetric data, we recommend using the Schwiderski maps of all constituents as a basis for computing currents.

7 Description of computer software

The foregoing analysis has been implemented in several Fortran-77 computer programs and subroutines, two of which warrant brief description in this section. The primary computational routine is a subroutine, `SHVEL`, which computes the in-phase and quadrature components of the south and east tidal currents (u_1, u_2, v_1, v_2) for a particular desired constituent, at a given

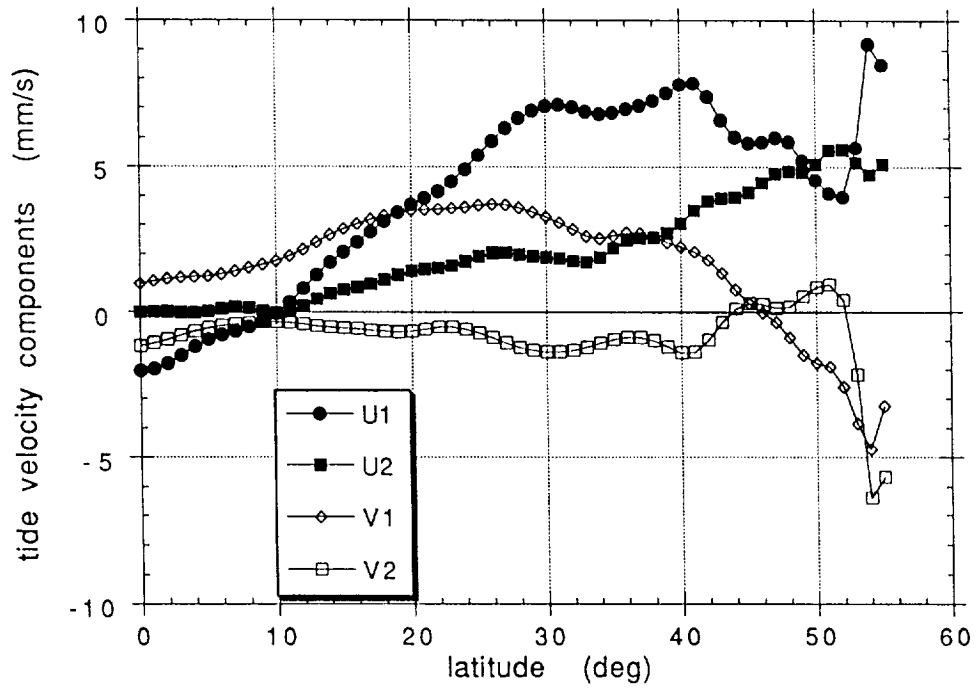


Figure 5: Cartesian components of the S_2 tidal currents along 140°W , computed from the tidal elevations of the Schwiderski numerical model.

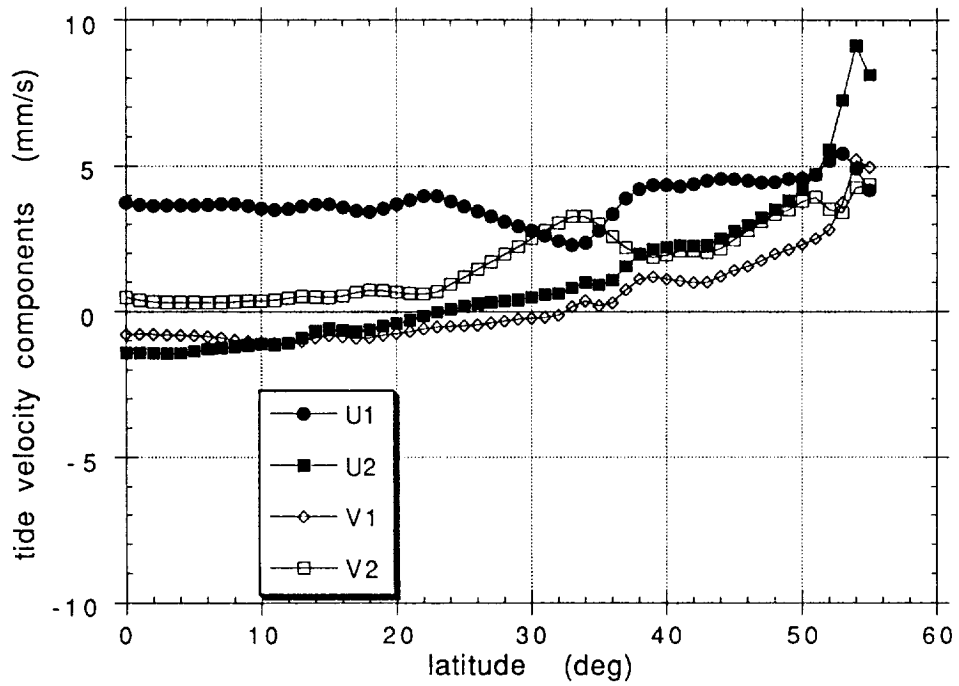


Figure 6: As in Figure 5, but for the O_1 constituent.

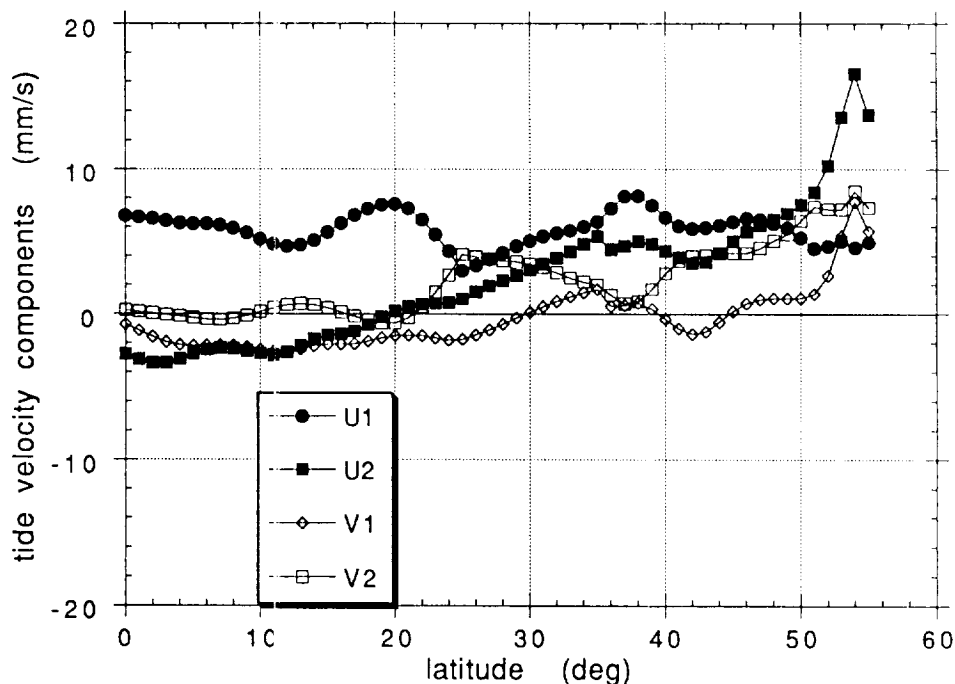


Figure 7: As in Figure 5, but for the K_1 constituent.

geographical position, and for a particular degree of expansion N' . The other routine is a small driver program plus associated routines that use the output of SHVEL for the eight major diurnal and semidiurnal tides, and, for a given time, predicts the total instantaneous tidal current. Routine SHVEL can obviously be used in any number of other applications, *e.g.*, to compute and plot rotary current vectors r^+ and r^- as in Figures 1 and 2.

SHVEL requires a number of input files. To compute γ'_n in equation (3), it requires a file of loading Love numbers h'_n and k'_n , complete to degree $n = N'$. It requires as well one or more files of spherical harmonic coefficients a_n, b_n, c_n, d_n , depending on which tidal constituent has been requested by the calling program. Each input file is read on a separate logical unit.

The prediction program SHVPRED calls SHVEL for each of the eight major tides and uses the resulting in-phase and quadrature velocity components to compute the total tidal current in mms^{-1} at any given time. In addition to the files requires by SHVEL, it requires a list of desired positions and times at which the tidal current is to be computed.

The software has been written in single precision, but we recommend converting to double precision on any machine with a short wordsize; often-times this can be done automatically by a simple compiler directive. The

software has been successfully executed on a Cray Y-MP, although it is not particularly well vectorized.

8 Conclusions

Our computer software for tidal currents in terms of the high-degree spherical harmonic expansion of surface elevations has been shown to give satisfactory results for the M_2 constituent at places where adequate measurements have been taken and in comparison with the currents extracted by E. W. Schwiderski from his dynamic model of M_2 . The same procedure applied to the Cartwright-Ray model derived from Geosat altimetry gives similar results in the longer wavelengths, but also shows short wavelength structure not present in the Schwiderski model, probably due to shortwave noise. This noise problem is more marked in the O_1 harmonic, and renders the Cartwright-Ray model of the diurnal tides unsuitable for accurate determination of currents. However, results from all major constituents of the Schwiderski model appear reliable, and probably give a total prediction with rms errors in the region $5\text{--}10\text{ mm s}^{-1}$ in the open ocean.

Within about 400–500 km of a coastline, results from our method appear erratic and are probably unreliable, even with the smooth Schwiderski maps. In these shelf sea regions it is probably necessary to construct a dynamic model with detailed bathymetry, and boundary conditions governed by the oceanic model together with coastal elevations.

Acknowledgments: We thank T. A. Herring (MIT) for providing the M_2 current components from Schwiderski's tide model (M_2 now being the only constituent extant). Figures 1–3 were created with the GMT plotting package, which was written by Paul Wessel (Univ. Hawaii) and Walter Smith (Scripps, UCSD).

REFERENCES

- Brosche, P., J. Wunsch, J. Campbell, and H. Schuh, Ocean tide effects in Universal Time detected by VLBI, *Astron. Astrophys.*, **245**, 676–682, 1991.
- Cartwright, D. E. and R. D. Ray, Oceanic tides from Geosat altimetry, *J. Geophys. Res.*, **95**, 3069–3090, 1990.
- Cartwright, D. E. and R. D. Ray, Energetics of global ocean tides from Geosat altimetry, *J. Geophys. Res.*, **96**, 16897–16912, 1991.
- Cartwright, D. E., R. D. Ray, and B. V. Sanchez, Oceanic tide maps and spherical harmonic coefficients from Geosat altimetry, NASA Tech. Memo. 104544, Goddard Space Flight Center, Greenbelt, 74 pp., 1991.
- Cartwright, D. E. and R. J. Tayler, New computations of the tide-generating potential, *Geophys. J. R. astr. Soc.*, **23**, 45–73, 1971.
- Farrell, W. E., Deformation of the Earth by surface loads, *Rev. Geophys. Space Phys.*, **10**, 761–797, 1972.
- Luyten, J. R. and H. M. Stommel, Comparison of M_2 tidal currents observed by some deep moored current meters with those of the Schwiderski and Laplace models, *Deep-Sea Res.*, **38**, S573–S589, 1991.
- Munk, W. H. and A. M. G. Forbes, Global ocean warming: an acoustic measure? *J. Phys. Oceanogr.*, **19**, 1765–1773, 1989.
- Olver, F. W. J. and J. M. Smith, Associated Legendre functions on the cut, *J. Comput. Phys.*, **51**, 502–518, 1983.
- Schwiderski, E. W., Ocean tides: I—Global ocean tidal equations; II—A hydrodynamic interpolation model, *Marine Geodesy*, **3**, 161–217 and 219–255, 1980.
- Schwiderski, E. W., Atlas of ocean tidal charts and maps: Parts II–XI, NSWC Tech. Repts., Naval Surface Weapons Center, Dahlgren, VA, 1983.
- Weisberg, R. H., D. Halpern, T. Y. Tang, and S. M. Hwang, M_2 tidal currents in the eastern equatorial Pacific Ocean, *J. Geophys. Res.*, **92**, 3821–3826, 1987.

REPORT DOCUMENTATION PAGE

Form Approved
OMB No. 0704-0188

Public reporting burden for this collection of information is estimated to average 1 hour per response, including the time for reviewing instructions, searching existing data sources, gathering and maintaining the data needed, and completing and reviewing the collection of information. Send comments regarding this burden estimate or any other aspect of this collection of information, including suggestions for reducing this burden, to Washington Headquarters Services, Directorate for Information Operations and Reports, 1215 Jefferson Davis Highway, Suite 1204, Arlington, VA 22202-4302, and to the Office of Management and Budget, Paperwork Reduction Project (0704-0188), Washington, DC 20503.

1. AGENCY USE ONLY (Leave blank)		2. REPORT DATE December 1992	3. REPORT TYPE AND DATES COVERED Technical Memorandum	
4. TITLE AND SUBTITLE A Computer Program for Predicting Oceanic Tidal Currents			5. FUNDING NUMBERS 926	
6. AUTHOR(S) D. E. Cartwright, R. D. Ray, and B. V. Sanchez				
7. PERFORMING ORGANIZATION NAME(S) AND ADDRESS(ES) Goddard Space Flight Center Greenbelt, Maryland 20771			8. PERFORMING ORGANIZATION 93B00032	
9. SPONSORING/MONITORING AGENCY NAME(S) AND ADDRESS(ES) National Aeronautics and Space Administration Washington, D.C. 20546-0001			10. SPONSORING/MONITORING AGENCY REPORT NUMBER TM-104578	
11. SUPPLEMENTARY NOTES D. E. Cartwright and R. D. Ray: Hughes STX Corporation, Lanham, Maryland.				
12a. DISTRIBUTION/AVAILABILITY STATEMENT Unclassified-Unlimited Subject Category 48			12b. DISTRIBUTION CODE	
13. ABSTRACT (Maximum 200 words) A computer model is developed for predicting depth-averaged tidal currents from a high-degree spherical harmonic expansion of the elevation field for any diurnal or semidiurnal harmonic constituent. Local friction is ignored, but loading and self-attraction potentials are fully allowed for by use of sequences of Love numbers. Critical latitudes for diurnal tides are covered by direct evaluation of the cyclonic component of current, and linear interpolation of the anti-cyclonic component within $\pm 5^\circ$ of latitude. Results agree reasonably well with selected measurements of M_2 currents and with M_2 currents computed within Schwiderski's model. However, the Cartwright-Ray model apparently gives noisier results for M_2 and is unacceptably noisy for diurnal constituents. Predictions from either model become unreliable within about 500 km of the coast, but in the open ocean, use of our method applied to the Schwiderski maps probably yields a prediction accuracy in the region of 5-10 mm/s ⁻¹ .				
14. SUBJECT TERMS Tides, Tidal Currents, Laplace's Tidal Equations			15. NUMBER OF PAGES 25	
			16. PRICE CODE	
17. SECURITY CLASSIFICATION OF REPORT Unclassified	18. SECURITY CLASSIFICATION OF THIS PAGE Unclassified	19. SECURITY CLASSIFICATION OF ABSTRACT Unclassified	20. LIMITATION OF ABSTRACT Unlimited	